

Robust Mode-Selection in Optical Bottle Microresonators

Ming Ding*, G. Senthil Murugan, Gilberto Brambilla, James S. Wilkinson, Michalis N. Zervas

Optoelectronics Research Centre, University of Southampton, Southampton, SO17 1BJ, UK

** Corresponding author: md20g09@orc.soton.ac.uk*

Abstract: We have demonstrated a robust and accurate method of selecting whispering gallery modes in optical bottle microresonators (BMR) by inscribing scars on BMR's surface by focused ion beam milling. A "cleaned-up" transmission spectrum was obtained after microstructuring.

OCIS codes: (140.4780) Optical resonators; (140.3948) Microcavity devices; (220.4241) Nanostructure fabrication;

1. Introduction

Optical microresonator based devices have recently attracted considerable attention, promising an increasingly wide range of applications [1]. Among microresonators, microdisks [2], microspheres [3] and microtoroids [4] rely on the efficient excitation of whispering gallery modes (WGM), which are confined predominantly in one azimuthal plane and show well resolved spectral characteristics. In contrast, a recently proposed truly 3-D optical microresonator, namely the bottle microresonator (BMR) [5]-[8], exhibits particularly dense spectral features, which require considerable effort to be identified [8]. The rich spectral features are a result of the strongly broken degeneracy between WGMs with common azimuthal and differing axial mode numbers, as a result of the highly prolate shape. While dense spectral features are highly advantageous when bottle microresonators are used in cavity QED studies [7], they can potentially be a serious hindrance if BMRs were to be used in other applications such as refractometric optofluidic sensors. In this case, a cleaner spectrum with more easily identifiable and traceable spectral features would be desirable. Exploiting the distinctly different spatial intensity distributions of the non-degenerate resonances supported by such highly non-spherical microresonators, different approaches, such as using high-index prisms [9] and micro-droplets [8], have been used to differentially attenuate modes and clean-up the spectrum. However, these techniques are cumbersome, not accurately controlled and difficult to integrate in practical systems.

In this paper, we introduce for the first time an accurately placed and controlled micro-scar on the surface of the BMR, using high-precision focused ion beam (FIB) milling, to clean up the original dense spectrum. This localized damage on the BMR's surface preferentially attenuates a subset of the bottle modes. Uniquely to this method, the shape, size and orientation of the scars can be controlled for optimum spectral clean-up. In addition, more than one micro-scar can be optimally placed in order allow only one bottle mode to survive.

2. Device Fabrication and Characterization

The "soften-and-compress" solid BMR fabrication technique [6] was employed to produce robust resonators. In this work, a standard telecom fiber (Corning SMF28) was used to fabricate BMRs with estimated neck-to-neck distance $L_b=350\ \mu\text{m}$, bottle diameter $D_b=170\ \mu\text{m}$ and stem diameter $D_s=125\ \mu\text{m}$. In previous work using similar microresonators [8], the radial penetration depth of the observed resonant modes was found to be about $6\ \mu\text{m}$.

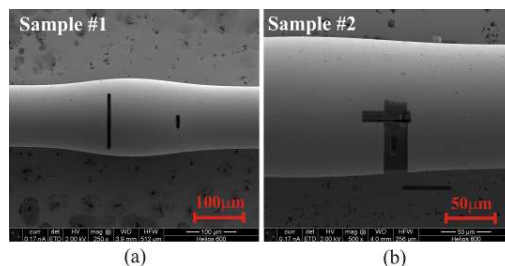


Fig. 1: FIB-milled scars on BMRs: (a) sample #1 with two scars perpendicular to the axis; (b) sample #2 with one scar parallel to the axis.

Scars of different sizes and orientations were carved using the FIB system "Helios 600" (FEI Inc., Hillsboro, USA). FIB beam sizes smaller than $50\ \text{nm}$ can be easily obtained, thus scar sizes can be controlled with excellent precision. Fig. 1 shows the SEM images of the gold-coated FIB-milled BMRs. In sample #1 (Fig. 1(a)) two scars were milled perpendicularly to the resonator axis and placed asymmetrically with respect to the BMR center. The first scar, with $5\ \mu\text{m}$ width, $109\ \mu\text{m}$ length and $6\ \mu\text{m}$ depth, was placed $50\ \mu\text{m}$ away from the center. The second scar, with $5.5\ \mu\text{m}$ width, $27.5\ \mu\text{m}$ length and $6\ \mu\text{m}$ depth, was placed $83\ \mu\text{m}$ away from the center. In sample #2 (Fig. 1(b)), a single scar, with $5\ \mu\text{m}$ width, $50\ \mu\text{m}$ length and $6\ \mu\text{m}$ depth was carved parallel to the BMR axis and placed $50\ \mu\text{m}$ away from the center. The gold coating was removed after FIB milling was completed.

BMRs were evanescently excited by a tapered fiber with waist diameter of $\sim 2 \mu\text{m}$ using a 100 kHz linewidth, tunable laser (Agilent 81600B). The tapered fiber was in contact with and perpendicular to the axis of the BMR, and placed at various positions along the axis. Fig. 2(a-d) shows the transmission spectra of sample #1. The transmission spectrum of the pristine BMR is also shown for comparison.

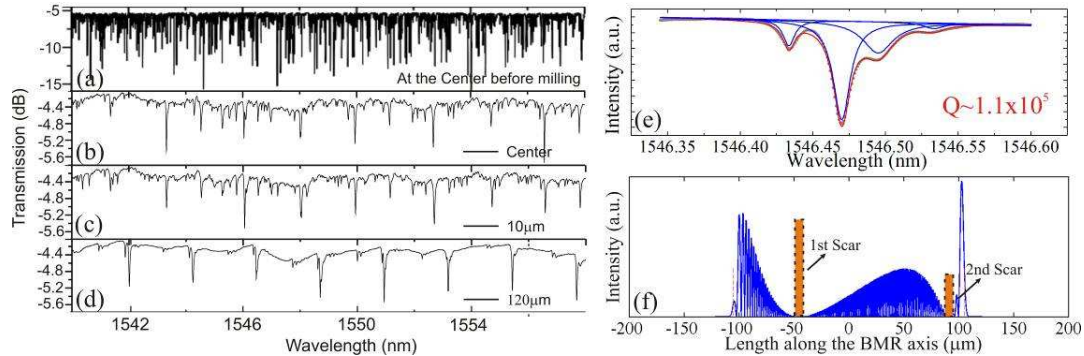


Fig. 2 (a) Transmission spectra of the tapered fiber-coupled #1 BMRs excited at the microresonator center (a) before microstructuring, after microstructuring at (b) the center; (c) 10 μm off-center; (d) 120 μm off-center; (e) Lorentzian fitting to a resonance group in Fig. 2 (d); (f) intensity distribution along the BMR axis when two modes are excited simultaneously.

Before FIB milling, rich and dense spectral characteristics are shown in Fig. 2(a) with the tapered fiber in the center of the BMR. In this case, all BMR modes can be potentially excited with amplitude that depends on their coupling strength with the micro-taper mode. Similarly dense spectra were obtained with the tapered fiber in different positions along the BMR length [6][8]. Fig. 2(b) and (c) show the corresponding spectra when WGMs in sample #1 are excited with the microtaper placed at the center and 10 μm off-center, respectively. It is shown that the spectra of the scarred BMR are substantially cleaner. As in the case of localized diffractive losses [8][9], this is due to the fact that only BMR modes concentrated around the resonator center survive with minimum losses, while modes which overlap or extend beyond the FIB scars experience severe scattering losses and are not excited efficiently. When the tapered fiber was placed beyond the region with two scars no sharp transmission resonances were observed. However, for a tapered-fiber position $\sim 120 \mu\text{m}$ from the center, shown in Fig. 2(d), sharp and well resolved periodic transmission notches appeared again. This is a unique feature of the two asymmetrically placed perpendicular scars of sample #1 and was not observed in the case of the long longitudinal scar of sample #2 or the diffractive localized loss in Ref. [8]. Fig. 2(e) shows that each of the resonance groups of Fig. 2(d) constitutes several partially-overlapping Lorentzian resonances. Fig. 2(f) shows the intensity distribution along the BMR length when two bottle modes are excited simultaneously. The mode beating results in broad-enough power minima in two places along the length. When these minima coincide with the scars the effects of the scattering loss is minimized and the sharp resonances re-appear. In this way, well defined individual groups of modes, with large axial mode number, occupying a large section of the BMR can be efficiently excited. It should be noted that each mode alone would not have “tunneled” through the scars and survived, since their power minima (anti-nodes) occur over areas much narrower than the scar width ($\sim 5 \mu\text{m}$). Such modes are expected to play important role in sensing applications.

4. Summary - Conclusions

In conclusion, we have presented an efficient, controllable and robust method of cleaning-up dense optical spectra in BMRs, using high precision FIB techniques. We have also demonstrated that a reduced group of modes can be predominantly selected with high-Q factor in BMRs with two asymmetrical scars. The shapes and positions of the milled scars can be chosen according to the application and the performance of microstructured BMRs can be improved by optimizing the scar shape size and orientation. This technique can be employed to clean up spectra in other types of non-spherical micro-resonators [4][9][10].

5. References

- [1] K. J. Vahala, “Optical Microcavities”, Nature **424**, pp. 839 (2003).
- [2] B. Gayral, et al, “High-Q wet-etched GaAs microdisks containing InAs quantum boxes”, Appl. Phys. Lett. **75**, pp. 1908 (1999).
- [3] D. W. Vernooy, et al, “High-Q measurements of fused-silica microspheres in the near infrared”, Opt. Lett. **23**, pp. 247 (1998).
- [4] D. K. Armani, et al, “Ultra-high-Q toroid microcavity on a chip”, Nature **421**, pp. 925 (2003).
- [5] M. Sumetsky, “Whispering-gallery-bottle microcavities: the three-dimensional etalon,” Opt. Lett. **29**, pp. 8 (2004).
- [6] G. S. Murugan, et al, “Selective excitation of whispering gallery modes in a novel bottle microresonator”, Opt. Express **17**, pp. 11916 (2009).
- [7] M. Pollinger, et al, “Ultrahigh-Q Tunable Whispering-Gallery-Mode Microresonator”, Phys. Rev. Lett. **103**, 053901 (2009).
- [8] G. S. Murugan, et al, “Hollow-bottle optical microresonators”, Opt. Express **19**, pp. 20773 (2011).
- [9] A. A. Savchenkov, et al, “Mode filtering in optical whispering gallery resonators”, Electron. Lett. **41**, pp. 495 (2005).
- [10] M. Sumetsky, “Optical microbubble resonator”, Opt. Lett. **35**, pp. 898(2010).